Corrected 9 August 2010; see below

www.sciencemag.org/cgi/content/full/science.1187942/DC1

Supporting Online Material for

PTIP Promotes Chromatin Changes Critical for Immunoglobulin Class Switch Recombination

Jeremy A. Daniel, Margarida Almeida Santos, Zhibin Wang, Chongzhi Zang, Kristopher R. Schwab, Mila Jankovic, Darius Filsuf, Hua-Tang Chen, Anna Gazumyan, Arito Yamane, Young-Wook Cho, Hong-Wei Sun, Kai Ge, Weiqun Peng, Michel C. Nussenzweig, Rafael Casellas, Gregory R. Dressler, Keji Zhao, André Nussenzweig*

*To whom correspondence should be addressed. E-mail: andre_nussenzweig@nih.gov

Published 29 July 2010 on *Science* Express
DOI: 10.1126/science.1187942

This PDF file includes:

Other Supporting Online Material for this manuscript includes the following:
(available at www.sciencemag.org/cgi/content/full/science.1187942/DC1)

Table S1 (zipped Excel file)

Correction: The listing for table S2 has been corrected.

MATERIALS AND METHODS

Mice

Paxip1 conditional knockout mice were generated as previously described having exon 1 flanked with loxp sites (*S1*). *Cd19*$^{cre/cre}$ mice are described previously (*S2*). All experiments were performed with *Cd19*$^{cre/+}$*Paxip*$^{+/+}$ and *Cd19*$^{cre/+}$*Paxip*$^{fl/fl}$ mice, unless otherwise noted. All experiments were performed in compliance with the NIH Intramural Animal Care and Use program. Immortalized *Paxip*$^{-/-}$ and control MEFs were described previously (*S3*).

B cell cultures and retroviral transduction

B cells were isolated from spleens of 6- to 14-week old mice by immunomagnetic depletion with α-CD43 beads (Miltenyi Biotech) and stimulated with LPS (25 μg/ml; Sigma), α-IgD-dextran (2.5ng/ml; FinaBio), IL4 (5 ng/ml; Sigma), or IL5 (15ng/ml; BD Pharmingen) for 2-5 days as indicated. Recombinant mouse IL6 (R&D Systems) was supplemented at 1.6ng/ml as indicated. For retroviral transduction into immortalized MEFs and primary B cells, FLAG-tagged WT and W663R mutant PTIP (*S4*) were cloned into pMIGR1, which carries an IRES-GFP to label the infected cells. Statistical significance was determined by a two-tailed *t* test assuming unequal variance.

Western blotting

Whole cell lysates were prepared as previously described (*S5*) and 50-100ug lysate was separated on either 4-12% NuPAGE (Invitrogen) or 5% Tris-Glycine

SDS-PAGE. Antibodies were used at the following dilutions: rabbit α-PTIP 1μg/ml (*S4*); rabbit α-PTIP 1:1000 (Bethyl); rabbit α-SMC1 1:1000 (Novus); α-α-TUBULIN (Sigma) 1:10,000. AID protein levels were analyzed as previously described (*S6*).

Genomic instability and imaging

Cultured B cells were arrested at mitosis with 0.1 μg/ml colcemid (Roche) treatment for 1 hour and metaphase chromosome spreads were prepared following standard procedures. FISH was performed on slides with probes for Igh-Cα (from Cγ1 to 3' of Cα), chromosome 12, and telomere-repeat specific peptide nucleic acid (Applied Biosystems), and counterstained with DAPI. Metaphase images were acquired with an Axioplan2 upright microscope (Zeiss) and Metamorph software. MEFs were fixed in 4% paraformaldehyde and processed for immunofluorescence using mouse α-FLAG (Sigma), rabbit α-53BP1 (Novus), or mouse α-γ–H2AX (Upstate). Mutations at Sμ were analyzed as described previously (*S7*). Sμ-Sγ1 switch recombination junctions were analyzed as described previously (*S7*). Immunocytochemistry-FISH for 53BP1 and IgH was performed as described previously (*S8*). 53BP1/IgH co-localization analysis was performed by acquiring images using a confocal LSM 510 Meta microscope (Zeiss) equipped with a 63X N.A. 1.4 objective lens (Plan Apochromat; Zeiss). A z-stack series was collected for each slide to obtain foci in all relevant focal planes (LSM v4). 53BP1 foci-positive cells containing 2 IgH foci

were selected for each genotype and analyzed using co-localization software (Imaris 7.0; Bitplane).

Flow cytometry and cell sorting

Single cell suspensions of ACK-treated splenocytes were stained with α-B220-FITC or α -IgM-PE (BD Pharmingen). For proliferation assays, cells were labeled with 5μM CFSE on day zero and dye dilution was assessed on day 4. Cultured B cells were harvested and stained in single cell suspensions with α -B220-FITC, α –IgG1-biotin, α –IgG3-biotin, α –IgG2b-biotin, and/or α –CD138-APC followed by streptavidin-PE, where necessary. Cells were acquired with either a FACScan or a FACSCalibur (BD Pharmingen) or sorted with a FACSVantage (BD Pharmingen) along with CellQuest software using a PI negative live lymphocyte gate. Data were analyzed using FlowJo software (v. 7.2.4).

ChIP-Seq

Resting or 2 day stimulated B cells were harvested for chromatin preparation, and ChIP and Illumina sequencing was performed as described previously (*S9*). For histone modification ChIPs, cells were washed and digested with MNase to generate native mononuclesomal chromatin fragments. For Pol II, PTIP, ASH2, and RBBP5 (Bethyl) ChIPs, cells were treated with 1% formaldehyde for 10 minutes at room temperature to generate cross-linked chromatin. Chromatin from 10^7 cells was used for each ChIP experiment and DNA was quantified using PicoGreen (Invitrogen) prior to Illumina sequencing. The antibodies used and the total tag number obtained for each ChIP-Seq sample are listed in Table S2. The

specificities of all antibodies used have been tested and verified as previously described (*S3, S9, S10*). Sequence reads were aligned to the mouse genome (mm8 or mm9) using standard Illumina Pipeline Analysis and only non-identical uniquely mapped reads were retained. Sequence read numbers were summed into 200bp (or 400bp for Pol II/PTIP/ASH2) non-overlapping windows with read position shifted 75bp (or 150bp for Pol II/PTIP/ASH2) to represent the DNA fragment center. Output data from the pipeline was converted to browser extensible data (BED) files for viewing the data in the UCSC genome browser. Genomic regions with histone modification marks/PTIP/ASH2 binding were identified using SICER with an E-value of 500 (*S11*). ChIP-Seq data is presented from both BED files and SICER-processed BED files. Data from SICER-processed BED files have been normalized to total non-redundant tag counts, while other data have been similarly normalized after browser-viewing.

Regions displaying significant PTIP-dependent H3K4me3 were determined using SICER (E-value = 500) with a p-value $<10^{-9}$ for significant decreases in each individual experiment along with a four-fold cut-off for the average fold-change decrease. Regions displaying significant PTIP association were determined from the union PTIP islands of both WT and KO identified by SICER (E-value = 500) as candidate regions. A p-value of 10^{-4} as well as a two-fold cut-off was used to identify true significant PTIP associated regions, compared with KO as control. Regions displaying ASH2 association were determined using the same criteria, using IgG as control. PTIP and ASH2 binding across 5' and 3' gene ends and gene body regions was determined as

previously described (*S12*) using islands with significant PTIP and ASH2 association, respectively. Tag counts were normalized by the total number of bases in the genic regions.

qPCR

For RT-qPCR, total RNA was extracted using TRIzol reagent (Invitrogen), treated with DNA-free RNase-free DNase (Ambion), and reverse transcribed with random hexamers using SuperScript III First-Strand Synthesis SuperMix (Invitrogen), all according to manufacturer's instructions. qPCR was performed in 20μl reactions on cDNA using 100nM of each primer, SYBR Green PCR Master Mix (Applied Biosystems), and a 7900HT Fast Real-Time PCR System machine (Applied Biosystems). Conditions for qPCR were as follows: 50^{o}C 2min, 95^{o}C 10min, then 40 cycles of 95^{o}C 30sec, 60^{o}C 30sec, 72^{o}C 30sec. Specificity of all primers was determined using no template negative controls and by dissociation curve analysis. Serially diluted cDNA samples were used to estimate the efficiency of each PCR for quantity calculation. All further statistical analysis was calculated using the standard curve method according to manufacturer's instructions (ABI User Bulletin #2). The following oligos were used: μ spliced: (5'-CTCGGTGGCTTTGAAGGAAC-3' and 5'-TGGTGCTGGGCAGGAAGT-3') (*S7*); γ1 spliced: (5'- TCGAGAAGCCTGAGGAATGTG-3' and 5'-ATGGAGTTAGTTTGGGCAGCA-3') (*S7*); Hprt: (5'-TGCCGAGGATTTGGAAAAAGTG-3' and 5'-CACAGAGGGCCACAATGTGATG-3') (*S13*); GAPDH: (5'-TGAAGCAGGCATCTGAGGG-3' and 5'-

CGAAGGTGGAAGAGTGGGAG-3') (*S7*); Paxip: (5'-GCAGCAGCAGCAGCTTTTTG-3' and 5'- TGCTCGGGATAGTCCGCAAT-3'); Il6: (5'- CAACGATGATGCACTTGCAGA-3' and 5'-TGGTACTCCAGAAGACCAGAGGA-3'); γ3 initiating: (5'-TCAATCCTGTTGTTAGCCTGTGC-3' and 5'-GGTCTGAATGCTACCCCACACC-3'); γ1 initiating: (5'- GGGCAGGACCAAAACAGGAA-3' and 5'-TTTCCCTGCTGACCCCACTC-3'); γ3 spliced: (5'-GAGGTGGCCAGAGGAGCAAGAT-3' and 5'-AGCCAGGGACCAAGGGATAGAC-3'); ε spliced: (5'-GGCAGAAGATGGCTTCGAATA-3' and 5'-ACAGGGCTTCAAGGGGTAGA-3'); γ3 unspliced: (5'-CCTGGCATCCTTGTAGGACCAA-3' and 5'-TCACCGAGGATCCAGATGTGTC-3'); γ1 unspliced: (5'-AAGGTTTGGTCCTGTCCTGTCC-3' and 5'-AGATGGGGGTGTCGTTTTGG-3');

For DC-qPCR, assay was performed as described (*S14*) with the following oligos: *Nicotinic acetyl choline receptor (nAChR)*: (5'-ACCTTGTCTCACACACAACCTTATTC-3' and 5'-AAGTTGGGATGTAGCTTCCATTATG-3'); *Igh*-Sμ-Sγ1 switch junction: (5'-TTACAGGTCAAGACTGAGTAGAATC-3' and 5'-CTGTAAATGCTTCGGGTATTGG-3').

For ChIP-qPCR, DNA was amplified using similar methods as described above for qPCR with the following oligos: *Igh*-γ1: (5'-CATTCTGGGGGTTTCTGTGT-3' and 5'-CAGGAGTACAGCCAGGCTTC-3').

SUPPLEMENTAL RESULTS AND DISCUSSION

PTIP-dependent H3K4me3 and development The severe proliferation defects in PTIP deficient primary MEFs and embryonic stem cells (*S15*) as well as impaired global H3K4me3 in PTIP deficient brain tissue (*S16*) may together explain the embryonic lethality observed in *Paxip1*$^{-/-}$mice (*S15*). Similarly, PTIP-deficient flies have developmental defects and also display decreases in global H3K4me3 (*S17*). Different from its roles in embryogenesis, our data demonstrate that, in activated B cells, PTIP is dispensable for proliferation and, rather, promotes H3K4me3 at very few loci across the genome, suggesting that PTIP function in histone methylation can vary dramatically depending on developmental context. Moreover, our data suggest that PTIP is dispensable for any possible H3K4me events essential during early B cell development and that the vast majority of H3K4me3 marks induced during B cell activation are either mediated by other methylases or possibly by other components of the MLL3/MLL4 complex. Similar to roles of different MLL-like complexes during embryogenesis, the remarkable non-redundant PTIP function at the *Igh* locus indicates that, even in peripheral lymphocytes nearing terminal differentiation, there can be exquisite specificity to target H3K4me.

***Igh* switch regions as clustered gene segments lacking H3K4me3**

A recent study demonstrated that while most genes display H3K4me3 and Pol II at their promoters and exhibit transcription initiation, only a minority of the inactive genes which lack both Pol II and H3K4me3 show no transcription

initiation (*S18*). This rare class of genes, exemplified by the olfactory receptor genes in ES cells, tends to be localized within clusters of highly homologous genes (*S18*). The identity of factors recruited to these tightly repressed genes that determine the change to active chromatin marks and transcription initiation remains unclear. In resting B cells and non- B cell types (i.e. T cells, (*S19*)), the *Igh* switch regions are normally refractory to H3K4me3 and Pol II recruitment; only upon B cell stimulation and PTIP binding to the switch regions do they acquire the chromatin changes necessary to initiate transcription. Given that the *Igh* locus contains clustered and highly repetitive switch regions which are controlled by the 3'Eα enhancer (*S20*), we propose that *Igh* switch regions are another example of this tightly repressed gene class and require PTIP to alleviate regulatory mechanisms that ensure proper targeting and stability of the switch regions.

PAX5 as a candidate transcription factor for recruitment of the PTIP-associated methyltransferase complex

Based on the observations that PTIP can directly interact with the PAX2 transcription factor (*S21*) and mediate recruitment of H3K4me activity to a PAX2-dependent promoter (*S16*), we speculate that PTIP-mediated H3K4me results from direct interaction with DNA-binding transcription factors (fig. S15, step 1). Interestingly, the only member of the PAX family expressed in the B lymphoid lineage, PAX5, has putative binding sites near every *Igh* switch region (*S22*) and promotes production of serum IgG (*S23*). Consistent with PAX5 being a

candidate transcription factor for recruiting the PTIP complex to *Igh*, we observed a correlation of PAX5 binding by ChIP-qPCR at the *Igh*-γ1 TSS in LPS and IL-4 stimulation conditions which promote IgG1 CSR compared to LPS stimulation alone (fig. S16). However, the promoter region at *Igh*-ε, which displays PTIP-independent H3K4me3 and switch transcripts, also contains a putative PAX5 binding site (*S24*), indicating that recruitment of the PTIP complex is likely not solely mediated by PAX5. PAX5-deficient mice exhibit a complete block in early B cell development and show severely impaired B cell proliferation (*S23, S25*), suggesting additionally that PAX5 clearly has PTIP-independent functions.

Support for H3K4me3 promoting recruitment and/or stabilization of Pol II

In one model, PTIP-mediated H3K4me3 catalyzed at transcription start sites (fig. S15, step 2) could recruit acetylases and chromatin remodelers that alter chromatin structure, thereby promoting recruitment and/or stabilization of Pol II to initiate transcription (fig. S15, step 2). This model is supported by a number of observations. First, the H3K4me3 mark can directly interact with the chromatin remodelers CHD1 and NURF as well as histone acetylase complexes containing ING proteins (*S26, S27*). Second, the H3K4me3 mark can also directly interact with the TAF3 subunit of TFIID, an interaction suggested to be important for promoters lacking canonical core promoter DNA elements (*S28*). Indeed, the initiation regions of the *Igh*-γ3, γ1, and γ2b switch transcripts all lack well-defined TATA boxes, leaving the mechanism for directing transcription initiation at these genes unclear (*S29*). Third, the relatively few inactive promoters in human cells

which display H3K4me3 show increased histone acetylation and Pol II binding upon inhibition of HDAC activities compared with promoters lacking H3K4me3, suggesting that H3K4me3 may be an initiating chromatin event leading to Pol II association (*S12*).

SUPPLEMENTAL FIGURES AND TABLES

Fig. S1. (A) Scatter plot of H3K4me3 ChIP-Seq data comparing tag counts from islands in resting and LPS and α-IgD-dextran stimulated B cells. Dashed lines indicate 4-fold change. (B) Only a minority of LPS-induced H3K4me3 islands are found at known promoters compared with the total H3K4me3 islands in LPS stimulated B cells. Pie charts showing the distribution of islands classified as either a known promoter, within a gene body, or in an intergenic region. H3K4me3 is induced at *Il6* (C) and *Igh* switch regions (D) upon B cell stimulation. H3K4me3 ChIP-Seq profiles from resting or 2 day LPS+α-IgD-dextran stimulated B cells. (E) Upon B cell activation, H3K4me3 at *c-Myc* is similar while at *Aicda* is induced. PTIP does not regulate H3K4me3 or Pol II association at *Aicda* or *c-Myc* in stimulated B cells. H3K4me3 and Pol II ChIP-Seq profiles from resting or 2 day LPS+α-IgD-dextran stimulated B cells. Gene annotation from browser is below the profiles.

Fig. S2. (A) Western blot analysis of PTIP and αTUBULIN from B cells stimulated with LPS+α-IgD-dextran for 2 days. Multiple $Paxip^{\Delta/\Delta}$ lanes indicate different mice. (B) RT-qPCR analysis of PTIP transcripts from B cells stimulated under the indicated conditions for 3 days. (C) Numbers of $CD19^{+}$ B cells in the spleen. Mean and standard deviation shown from 11 mutant and 10 control mice ($p=0.1096$). (D) Flow cytometric analysis of splenocytes stained to indicate percent of total live IgM^{+} B cells. B220 is used as a pan B cell marker. Data are representative of 4 independent experiments. (E) Flow cytometric analysis of

carboxyfluorescein succinimidyl ester (CFSE)-labeled B cells cultured in the presence of either LPS+α-IgD-dextran (left) or LPS and IL4 (right) for 4 days. Data are each representative of 3 independent experiments.

Fig. S3. (A) ChIP-Seq scatter plot of H3K4me3 islands in PTIP-deficient LPS+α-IgD-dextran stimulated B cells indicates very few changes genome-wide. Dashed lines indicate 3-fold change. No consistently significant islands displaying H3K4me3 increases in *Paxip*$^{\Delta/\Delta}$ cells were observed across three independent experiments. (B) Table showing average fold change decrease of regions with more than a 3-fold change from three independent H3K4me3 ChIP-Seq experiments, as in Fig. 1A. The chromosome number and coordinates of islands are presented as indicated from the Feb 2006 (NCBI36/mm8) assembly of the mouse genome. Two separate PTIP-dependent H3K4me3 islands are observed at *Igh*-γ2b and have been grouped as a single region in the text for simplicity. The two islands may be the result of poor sequencing of the γ2b switch repeats.

Fig. S4. H3K4me3 at the *Igh* locus in response to LPS+IL4 stimulation. Above, PTIP-dependent H3K4me3 at the γ1 switch region. Below, H3K4me3 across the *Igh* locus is unchanged in *Aicda*$^{-/-}$ B cells suggesting that PTIP-dependent H3K4me3 at downstream switch regions occurs upstream of AID-induced DNA damage. H3K4me3 ChIP-Seq profiles from B cells stimulated for 2 days.

Fig. S5. (A) Flow cytometric analysis of CFSE-labeled B cells stimulated with

LPS and α-IgD-dextran (left) or LPS and IL-4 (right) for 4 days and stained with antibodies against IgG3 or IgG1. Numbers indicate percent of total live IgG^+ B cells. (B) Class-switching defects in *Paxip*$^{\Delta/\Delta}$ B cells are similar across multiple cell divisions in LPS+α-IgD-dextran (above) and LPS+IL4 (below) conditions. Percent IgG^+ B cells as a function of cell division based on CFSE dye dilution by flow cytometry. Data are each representative of 3 independent experiments. (C) DC-qPCR analysis of Sμ-Sγ1 recombination from genomic DNA of B cells stimulated with LPS+IL4 for 4 days. Data are representative of 2 independent experiments. *nAChR* is used as a control for variations in template amount and efficiencies in digestion and ligation. (D) Flow cytometric analysis of B cells stimulated with LPS and α-IgD-dextran for 4 days and stained with propidium iodide. Numbers indicate percent of total live lymphocytes. Data are representative of many independent experiments.

Fig. S6. Exogenous IL6 does not rescue IgG3 class-switching defect in *Paxip*$^{\Delta/\Delta}$ B cells. Flow cytometric analysis of B cells stimulated with LPS+α-IgD-dextran with or without recombinant mouse IL6 for 4 days and stained with α-IgG3. Numbers indicate percent of total live $IgG3^+$ B cells. Data are representative of 2 independent experiments.

Fig. S7. (A) Island score distribution histogram of the LPS+α-IgD-dextran--induced H3K4me3 islands from fig. S1A indicating that the *Igh*-γ3 island peak deviates from the normal distribution. Island scores were calculated based on

island peak width and total number of tags within an island. (B) H3K4me3 ChIP-Seq profiles across the γ3 region of the *Igh* locus in LPS+α-IgD-dextran 2 day stimulated B cells. (C) and (D) Above, illustrations showing location of oligos used in RT-qPCR. Below, RT-qPCR analysis of spliced (B) and unspliced (C) *Igh* switch transcripts from B cells stimulated under the indicated conditions for 3 days.

Fig. S8. Histone modifications, Pol II, PTIP, and ASH2 association at genes displaying PTIP-dependent H3K4me3, other than *Igh* switch regions. ChIP-Seq profiles in B cells stimulated with LPS+α-IgD-dextran for 2 days across the entire indicated gene. Gene annotation from the browser is below the profiles. Significant PTIP and ASH2 association are presented as fold change enrichment of island tag counts from control/ *Paxip*$^{\Delta/\Delta}$ and ASH2/ IgG, respectively. Locations of PTIP-dependent H3K4me3 are highlighted with orange boxes.

Fig. S9. H2BK5ac, H3K9ac, H3K4me2, and H3K4me1 ChIP-Seq profiles across the *Igh* constant region locus in B cells stimulated with LPS+α-IgD-dextran for 2 days. Data indicate that while H2BK5ac, H3K9ac, and H3K4me2 are deficient specifically at *Igh*-γ3 and γ2b switch regions, H3K4me1 is unchanged across the entire locus in *Paxip*$^{\Delta/\Delta}$ B cells.

Fig. S10. (A) Left, scatter plot of PTIP ChIP-Seq data comparing tag counts from islands in *Paxip*$^{\Delta/\Delta}$ (as control) and WT B cells stimulated with LPS+α-IgD-

dextran. Right, scatter plot of ASH2 ChIP-Seq data compared to tag counts from control rabbit IgG islands. For both plots, dashed lines indicate 2-fold decrease in tag counts from data normalized by total non-redundant sequence tags. Each data point represents an island. The data points below the dashed line are those showing a >2 WT/KO or ASH2/IgG ratio, respectively. Among them, 9,647 islands were identified with significant PTIP association and 27,806 islands with significant ASH2 association, determined with an additional cut-off of p-value < 10^{-4}. (B) Composite PTIP and ASH2 association profiles across genic regions. Data are from islands with significant PTIP or ASH2 association identified in (A). (C) PTIP associates with a minority of regions displaying LPS-induced H3K4me3, while ASH2 associates with the majority of these regions. Pie charts showing distribution of islands identified in fig. S1A as either associated or not associated with PTIP (above, left) or ASH2 (above, right). Below, of the LPS-induced regions associated with PTIP, ASH2 almost completely co-localizes.

Fig. S11. (A) ASH2 directly localizes to *Igh* in an LPS-dependent manner. ASH2 and control IgG ChIP-Seq profiles across the *Igh* constant region locus in B cells either stimulated with LPS and α-IgD-dextran for 2 days or with no stimulation. (B) PTIP, RBBP5, and H3K4me3 ChIP-qPCR results from B cells stimulated with LPS+IL4 for 2 days. Rabbit IgG is used as a negative control. Illustration shows location of *Igh*-γ1 oligos used in qPCR. (C) PTIP ChIP-qPCR results from MEFs with or without LPS+IL4 stimulation for 2 days. Rabbit IgG is used as a negative control. *Igh*-γ1 oligos used were same as in (B). Notice the difference in the y-

axis maximum compared with that in (B).

Fig. S12. No major changes in H3K4me3, Pol II association, or expression of CSR-related factors in *Paxip*$^{\Delta/\Delta}$ B cells. (A) H3K4me3 and Pol II sequence tags from ChIP-Seq data of B cells stimulated with LPS+α-IgD-dextran for 2 days were summed across the indicated gene bodies, including 1kb upstream and downstream of the gene. Data are normalized to total non-redundant tag counts for comparison. (B) RT-qPCR analysis of transcripts from B cells stimulated with LPS+α-IgD-dextran for 3 days. Mean and standard deviation shown from 2 mutant and 2 control mice.

Fig. S13. Switch recombination junctions are normal in *Paxip*$^{\Delta/\Delta}$ B cells. Shown are sequences of Sμ-Sγ1 switch junctions analyzed from genomic DNA of *Paxip*$^{\Delta/\Delta}$ and control B cells sorted for IgG1 surface expression after stimulation with LPS+IL4 for 3 days. Sμ sequence is in black and Sγ1 sequence is in gray. Sequence additions (green) and overlaps (red) are indicated. 17 *Paxip*$^{\Delta/\Delta}$ and 14 control sequences were analyzed.

Fig. S14. PTIP is dispensable for 53BP1 foci formation in MEFs. (Left) IF images of immortalized MEFs exposed to 2Gy IR with indicated recovery times showing 53BP1 and γ−H2AX foci formation. Bar, 20μm. (Right) Western blot analysis of PTIP and SMC1 loading control from MEFs. Two different PTIP antibodies were used. Arrow indicates PTIP, asterisk indicates non-specific reactivity.

Fig. S15. Model for the dual functions of PTIP during immunoglobulin CSR. In resting B cells, transcription initiates upstream of the V(D)J gene segment for full-length *Igh* transcript and from 5'Eμ to generate the μ sterile switch transcript, but is completely absent from the downstream cluster of switch regions and constant gene segments. After B cell activation (i.e. LPS stimulation), PTIP localizes to downstream γ switch regions (step 1) and promotes chromatin changes (step 2) leading to transcription initiation. Solid arrow indicates 'directly mediates' while dashed arrows indicate 'directly or indirectly mediates' association. Accessibility of AID to transcribed switch region chromatin targets AID activity to *Igh*, leading to DSB formation (step 3). BRCT domain-mediated and γ-H2AX/RNF8-dependent accumulation of PTIP at CSR-associated DSBs functions to suppress genomic instability and promote efficient CSR (step 4). TF, transcription factor.

Fig. S16. PAX5 associates near the *Igh*-γ1 TSS in B cells stimulated with LPS and IL-4 but not LPS and α-IgD-dextran. PAX5 and H3K4me3 ChIP-qPCR results from B cells stimulated for 2 days. Rabbit IgG and no antibody are used as negative controls.

Table S1. LPS-induced H3K4me3 regions. Islands identified in fig. S1A displaying a fold change of >4 and a p-value $<10^{-4}$. The chromosome number and coordinates of islands are presented as indicated from the Feb 2006 (NCBI36/mm8) assembly of the mouse genome.

Table S2. Total sequence tag counts and antibodies used in ChIP-Seq experiments. Superscript numbers in genotypes indicate experiments.

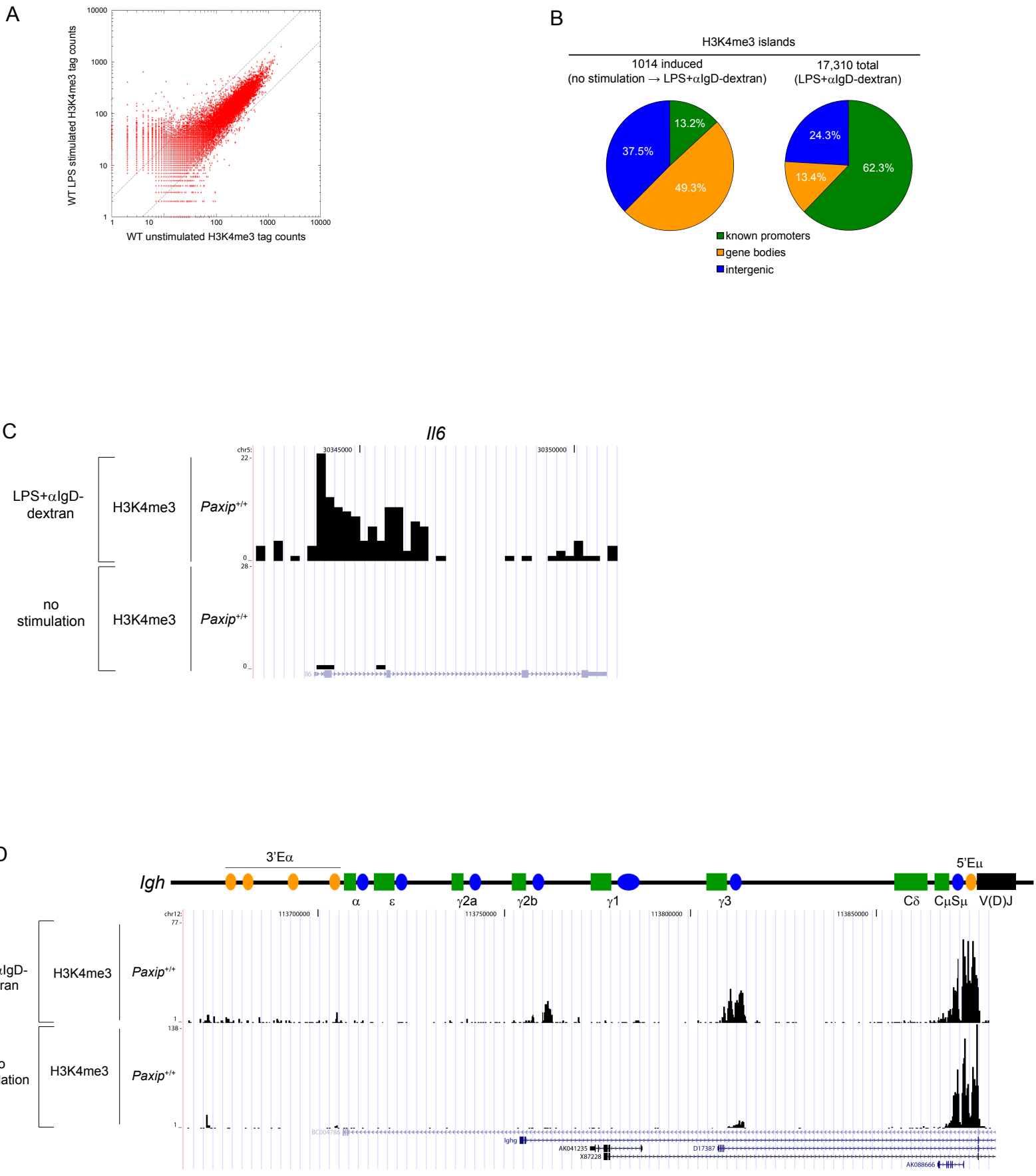

Supplementary Figure 1

E

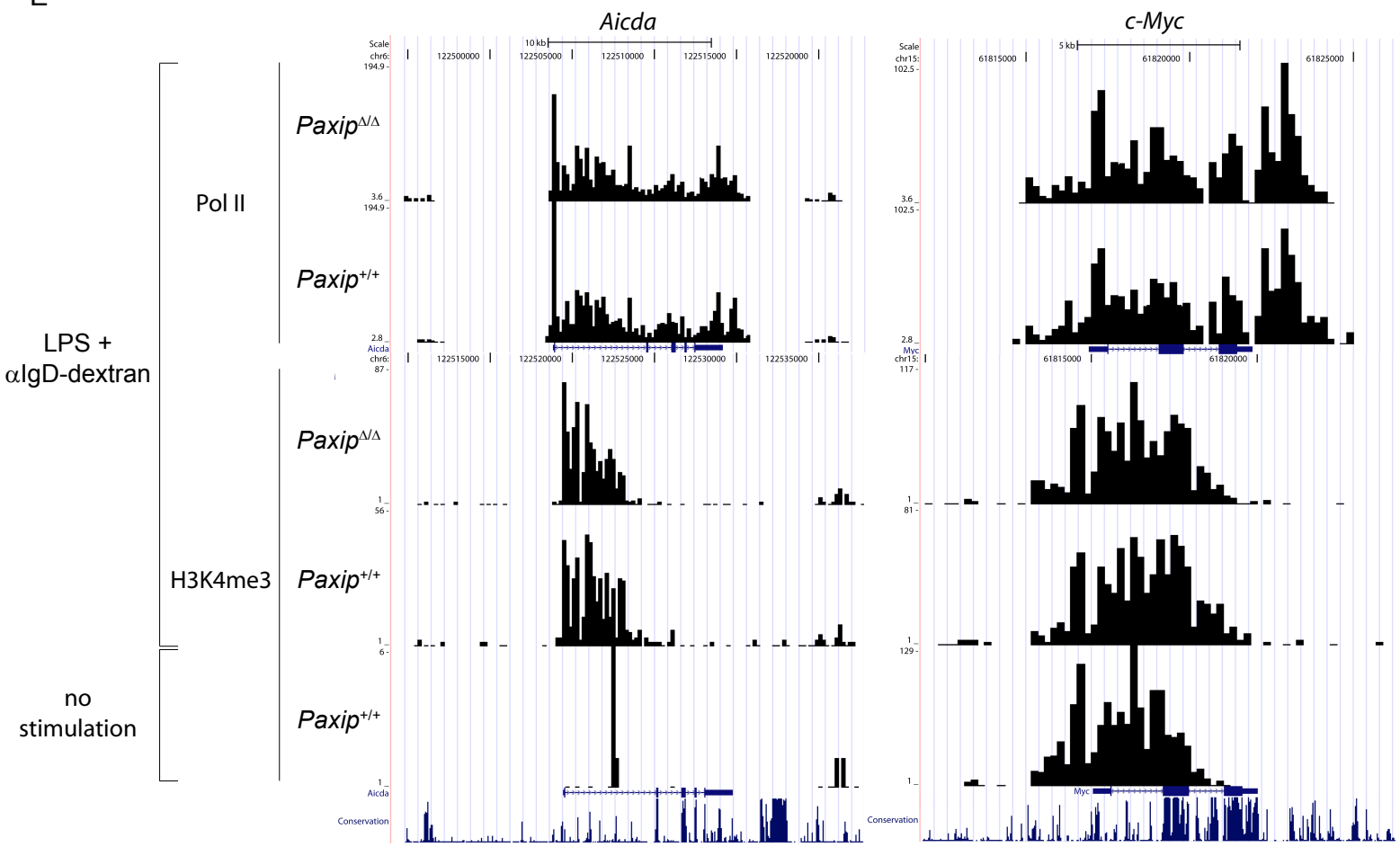

Supplementary Figure 1 continued

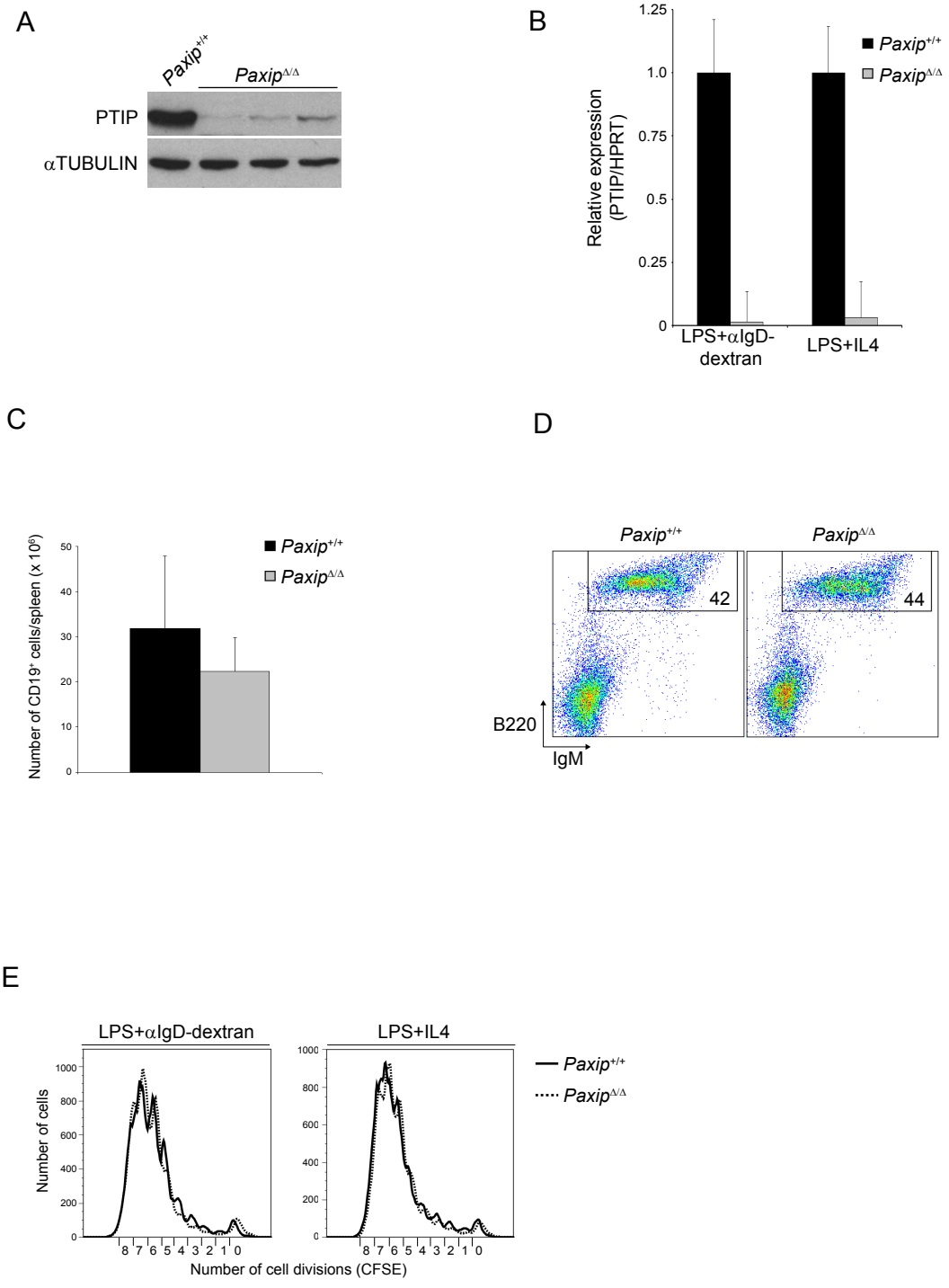

Supplementary Figure 2

A

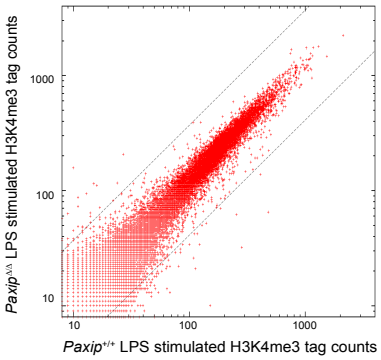

B

Regions displaying PTIP-dependent H3K4me3

Chr	Start	End	Region	Fold change
12	113755800	113758199	*Igh*-γ2b switch region	30.5
12	113808400	113814999	*Igh*-γ3 switch region	11.4
12	113760200	113762599	*Igh*-γ2b switch region	10.8
5	28120200	28124199	*Paxip*	8.9
11	34963800	34966999	*Slit3*	7.0
1	156644400	156647599	mRNA AK171983/*Cacna1e*	4.9
5	30343600	30346599	*Il6*	4.0
11	45903200	45906199	*Adam19*	3.9
18	60916800	60919199	*no annotation*	3.8
7	24171200	24172999	*Plaur*	3.4
1	137933000	137936399	*Cacna1s*	3.4

Supplementary Figure 3

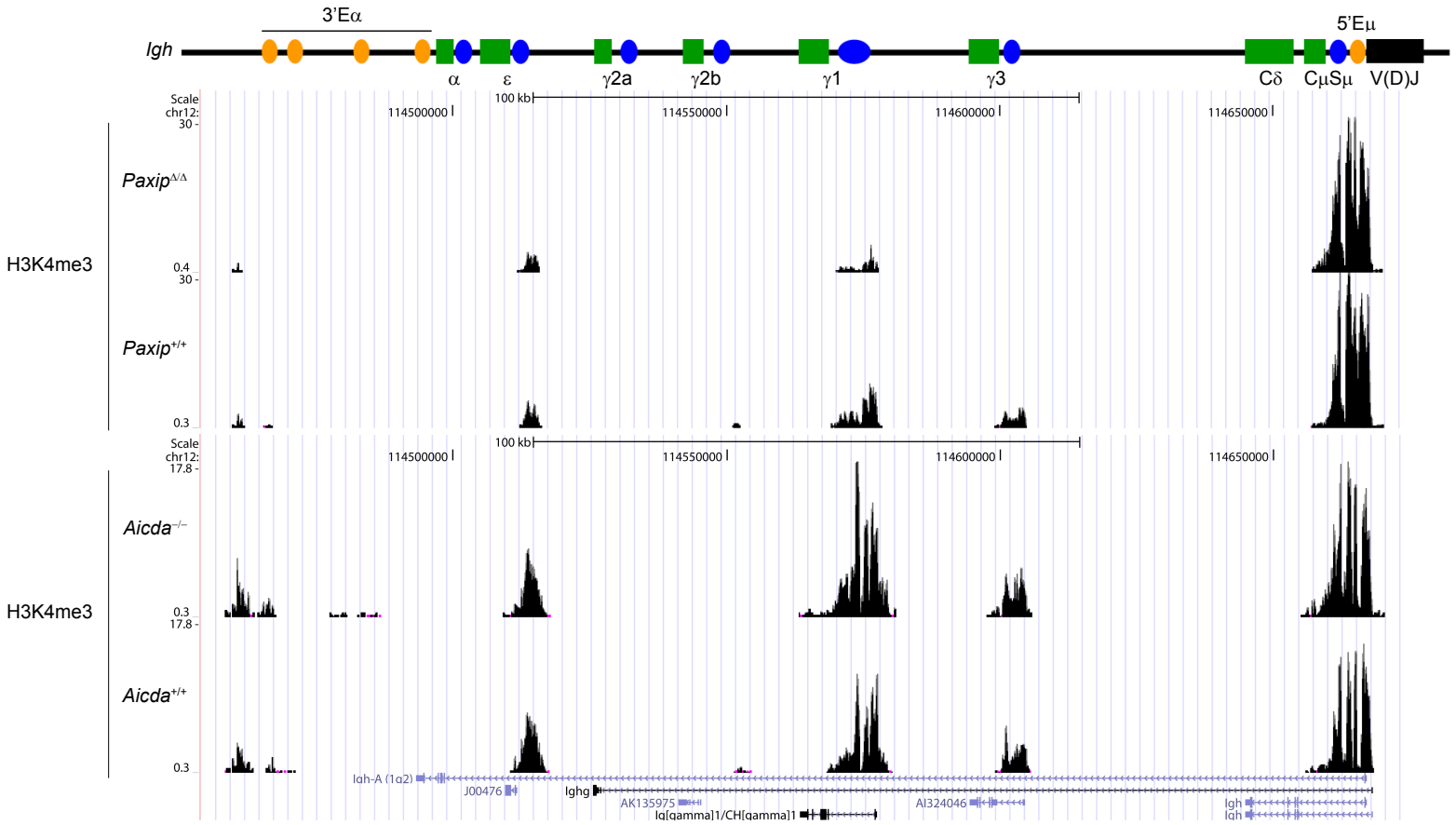

Supplementary Figure 4

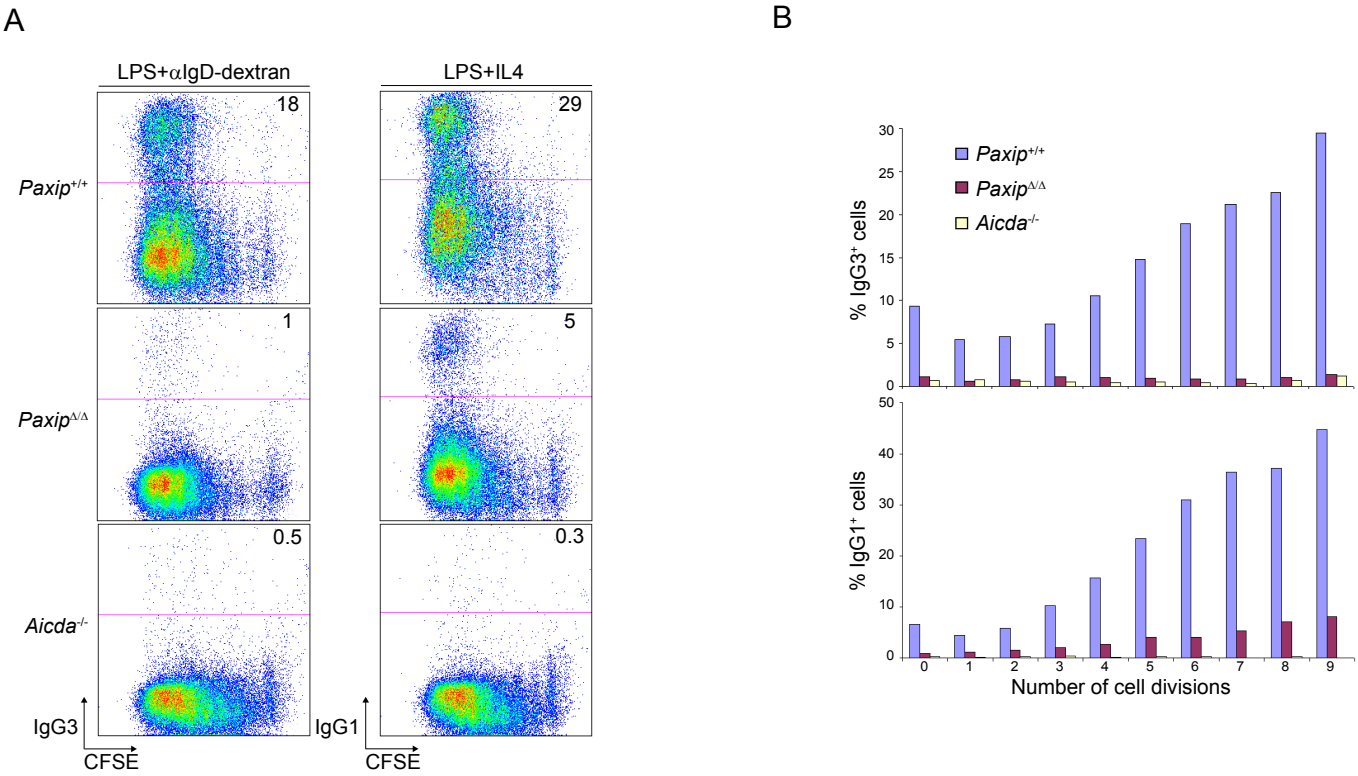

Supplementary Figure 5

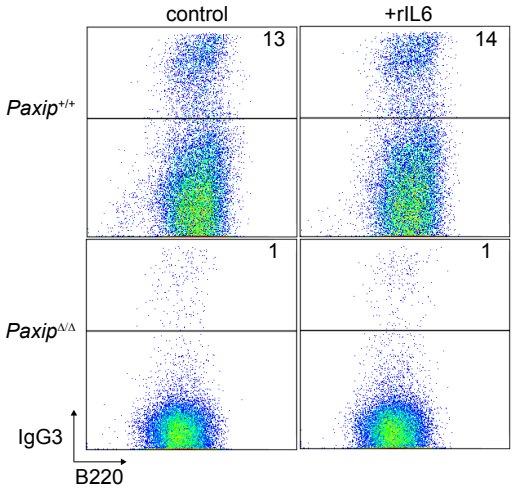

Supplementary Figure 6

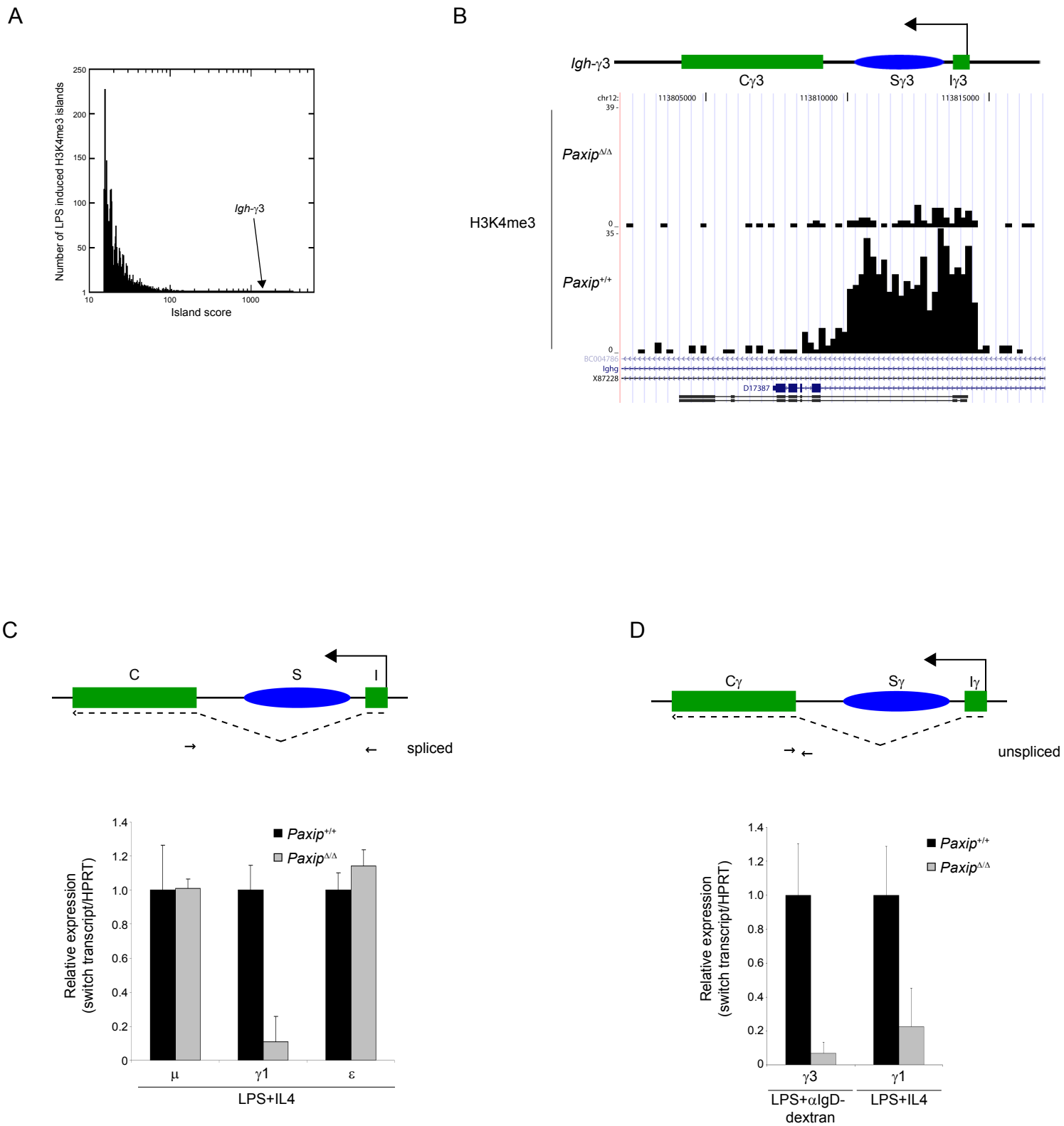

Supplementary Figure 7

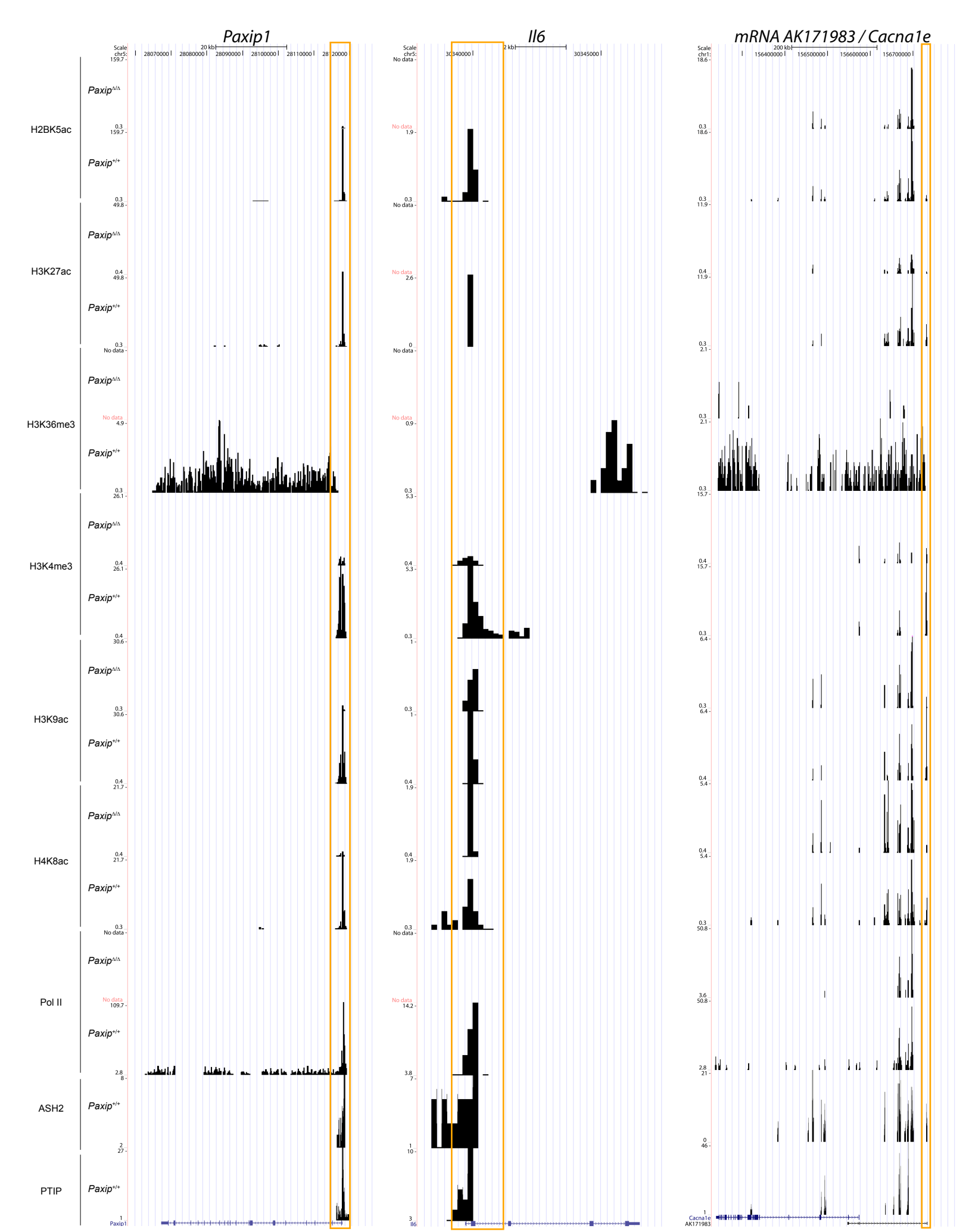

Supplementary Figure 8

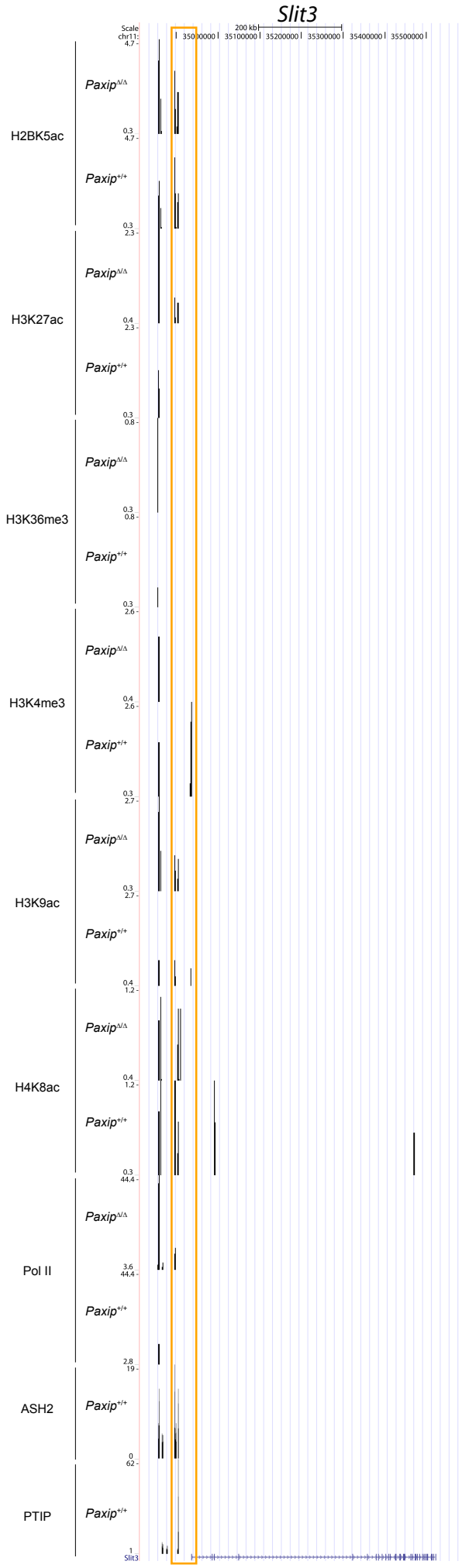

Supplementary Figure 8 continued

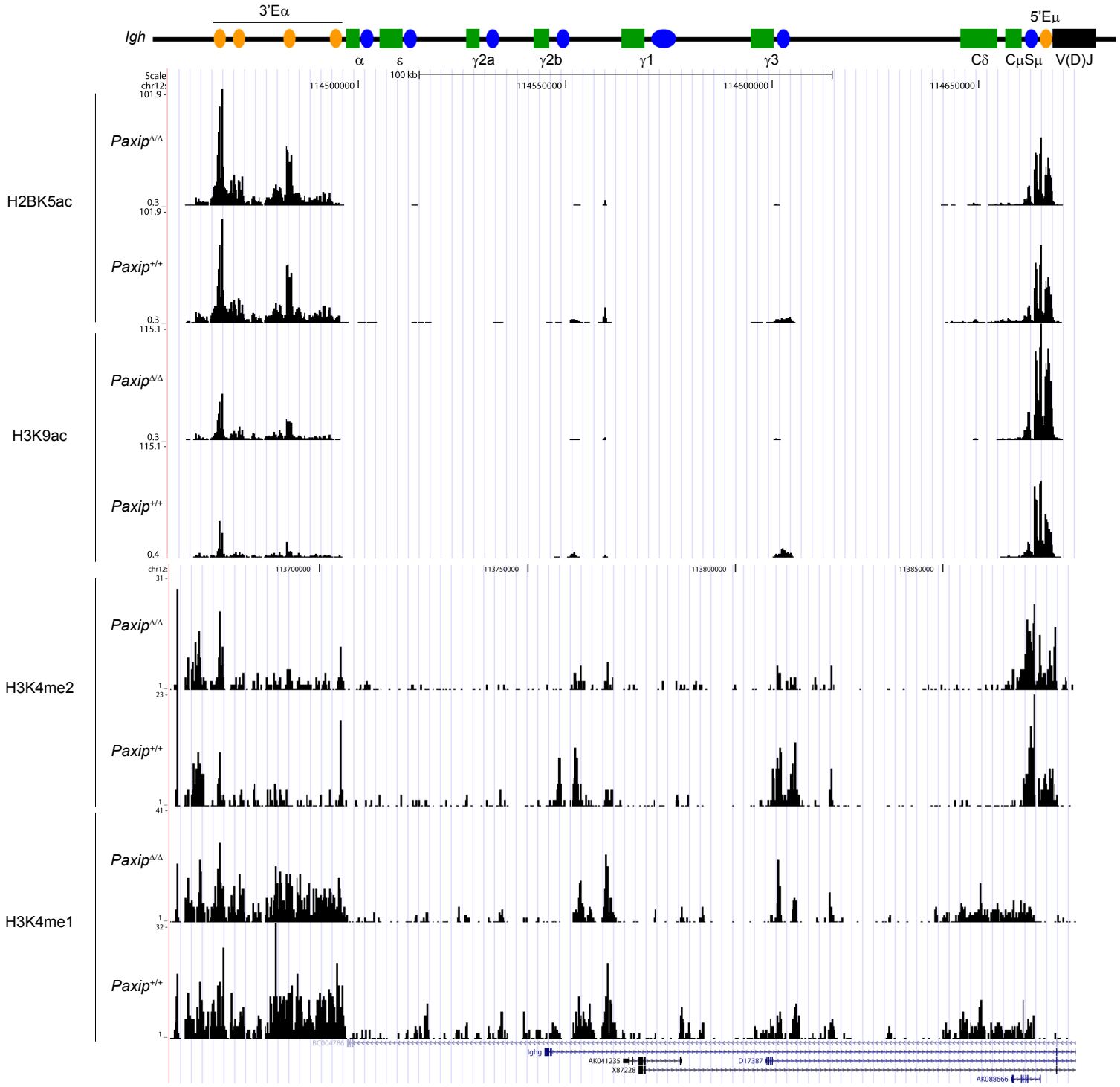

Supplementary Figure 9

A

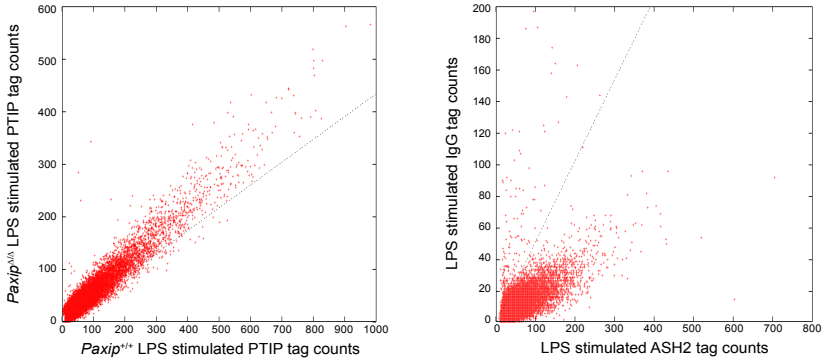

B

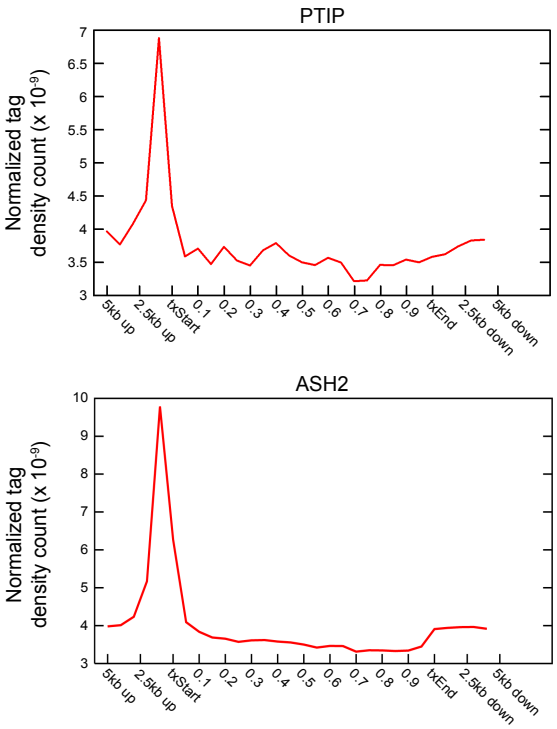

C

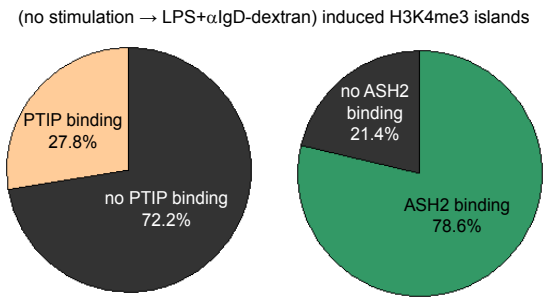

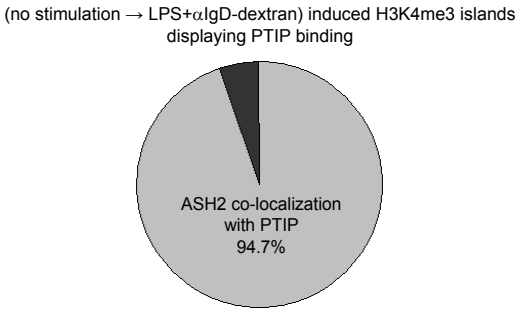

Supplementary Figure 10

A

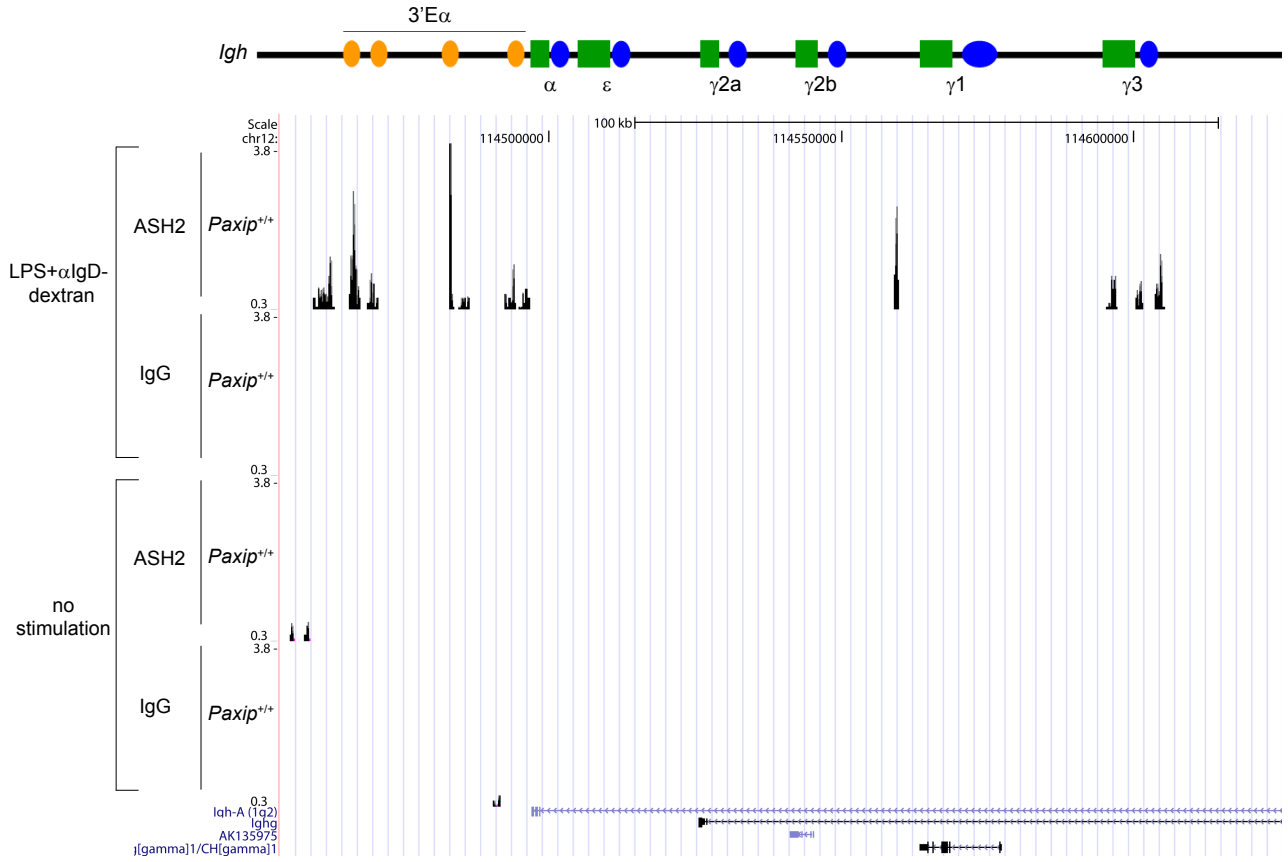

B

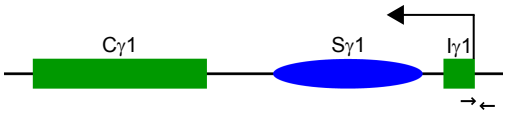

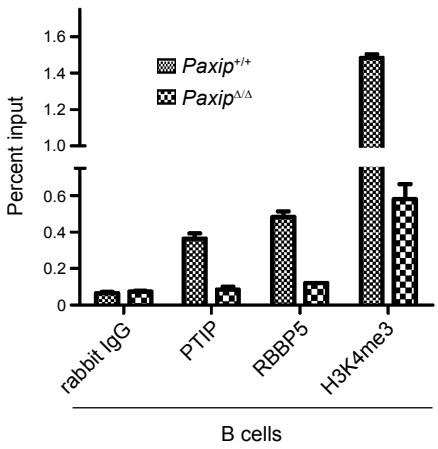

C

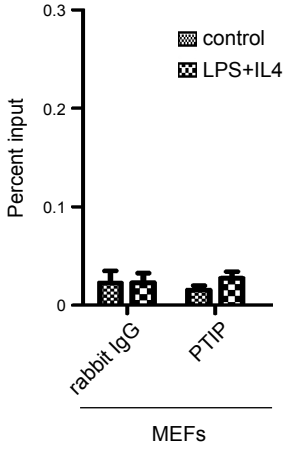

Supplementary Figure 11

A

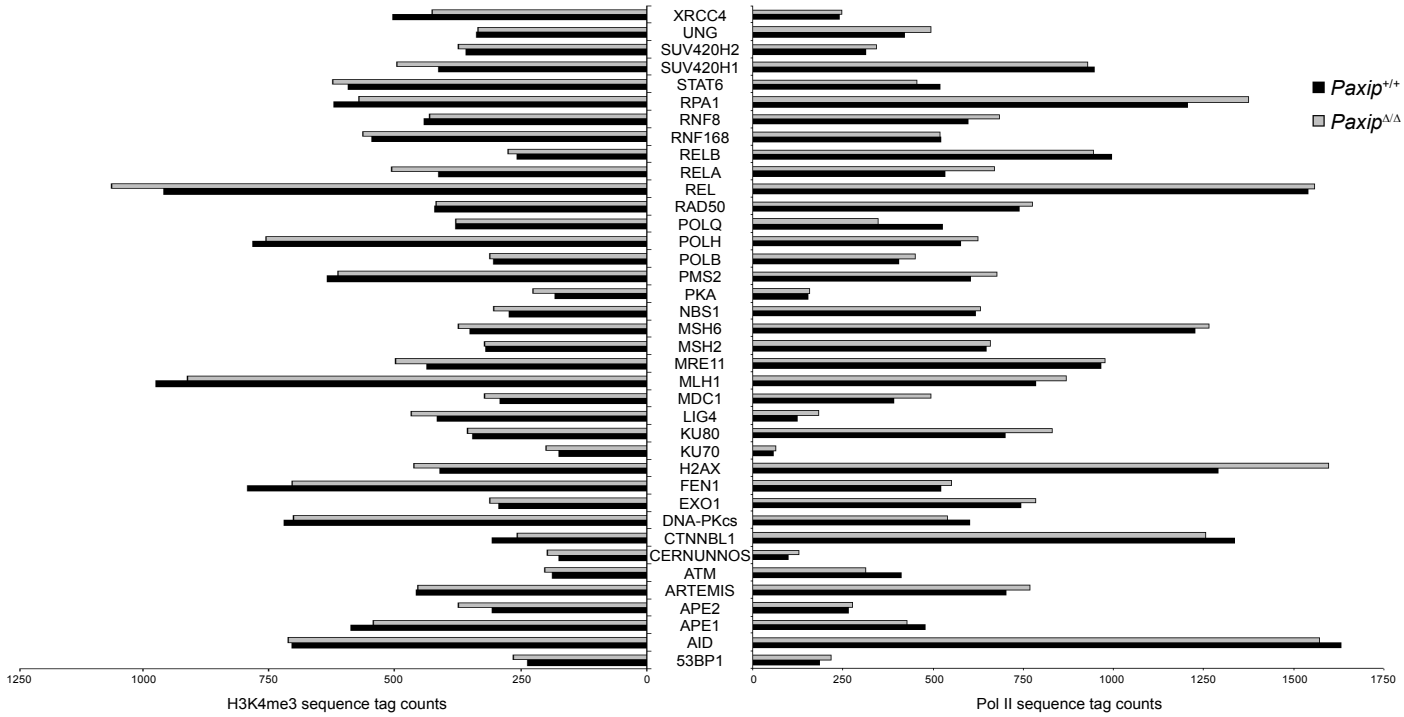

B

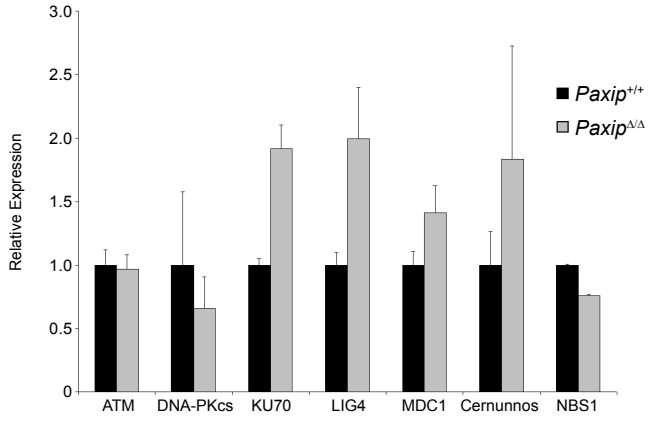

Supplementary Figure 12

Paxip$^{\Delta/\Delta}$ TGAGAGGACAGGGGCTGGGGTATATAGGGCAGCCAGGACAGGTGGGGGTGTGGGGATCCAGGTAA
Paxip$^{\Delta/\Delta}$ ATGGATACGCAGAAGGAAGGCCACAGCTGTGCAGCCAGGACAGGTGGGAGTGTGGGGATCCAGGT
Paxip$^{\Delta/\Delta}$ AATGTGGTTTAATGAATTTGAAGTTGCCAGTAAATTGAAGTGTAGTGCCTTGGGAGCCAGAACAGA
Paxip$^{\Delta/\Delta}$ GAAAAGATGTTTTTAGTTTTTATAGAAAGCAGGTACATACGGGTAAGCAGGAACAGGTGGAAGT
Paxip$^{\Delta/\Delta}$ TGGTTTAATGAATTTGAAGTTAGAGCAGCTATAGGGCAGCCAGGACAGGTGGGAGTGTGG
Paxip$^{\Delta/\Delta}$ GAGACCTGCAGTTGAGGCCAGCAGGTCGACTAGGGTGCCAGGACAGGTACAAGTTTAGTAGTT
Paxip$^{\Delta/\Delta}$ CTCAATGTGGTTTAATGAATTTGAAGTTAGAGCAGCTATAGGGCAGCCAGGACAGGTGGGAG
Paxip$^{\Delta/\Delta}$ GAGGACAGGGGCTGGGGTATGGATACGCAGAGGTGAGCAAATACAAGGGAACTGATGGCAAATG
Paxip$^{\Delta/\Delta}$ GACCTGCAGTTGAGGCCAGCAGGTCGGCTAGGGTGCCAGGACAGGTACAAGTTTAGTA
Paxip$^{\Delta/\Delta}$ AATCCTGGGATTCTGGAAGAAAAGAATCCAGTTGAGGTGGAAGAATGGGGATCCAGGCAGAGTAGC
Paxip$^{\Delta/\Delta}$ TATAGAAAACACTACTACATTCTCGATCTACAAAATACAAGGGAACTGATGGCAAATGAA
Paxip$^{\Delta/\Delta}$ TCCTGGTTGTTAAAGAATGGTATCAAAGGTGCTGCAGCTACATACGGGTAAGCAGGAACAGG
Paxip$^{\Delta/\Delta}$ TGAGCTGAGCTGAGCTGGGGTGAGCTGAGCAGATACAGGGAAGCTGAGGCAGGTAAG
Paxip$^{\Delta/\Delta}$ CAACTCAATGTGGTTTAATGAATTTGAAGTTAGAGCAGCTATAGGGCAGCCAGGACA
Paxip$^{\Delta/\Delta}$ CTAGGNTGANCTGGGCTGNNTGGGGTGANCTGANCTGANTGGGGTAGCTGAGGCAGGTAA
Paxip$^{\Delta/\Delta}$ TCCTGGTTGTTAAAGAATGGTATCAAAGGTGCTGCAGCTACATACGGGTAAGCAGGAACAG
Paxip$^{\Delta/\Delta}$ GGGCTTGAGCCAAAATGAAGTAGACTGTAGAGGAACAGGGGCAGGTTAGAATGAAGGATGT

Paxip$^{+/+}$ GCAATCCTGGGATTCTGGAAGAAAAGAATCCAGCTGAGGTGGAAGAATGGGGATCCAGGCAGAGTAGC
Paxip$^{+/+}$ CCTTGACCCAGGCTAAGAAGGCAATCCTGGGATTCTGGAAGAAAAGATGTTTTTAGTTTT
Paxip$^{+/+}$ GAGGACAGGGGCTGGGGTATGGATACGCAGAGGTGAGCAAATACAAGGGAACTGATGGCAAATG
Paxip$^{+/+}$ TTAAAGAATGGTATCAAAGGACAGGAGCAAGGACAGGGAAGCTATAGGGAAAC
Paxip$^{+/+}$ TGGAAGAAAAGATGTTTTTAGTTTTTATAGAATCGGGTAAGCAGGAACAGGTGGAAGTGTA
Paxip$^{+/+}$ GATTCTGGAAGAAAAGATGTTTTTAGTTTGGTGGAAGAATGGGGATCCAGGTGCTGCAG
Paxip$^{+/+}$ AATAGAGACCTGCAGTTGAGGCCAGCAGGTCGACTAGGGTGCCAGGACAGGTACAAGTTTAGT
Paxip$^{+/+}$ ACCTGCAGTTGAGGCCAGCAGGTCGGCTAGGGTGCCAGGACAGGTACAAGTTTAGTAGTT
Paxip$^{+/+}$ AAGTTGCCAGTAAATGTACTTCCTGGTTACAGAGAAGCTGAGGCAGGTAAGAGT
Paxip$^{+/+}$ AAAGATGTTTTTAGTTTTTATAGAAAGCAGGTACATACGGGTAAGCAGGAA
Paxip$^{+/+}$ GGATACGCAGAAGGAAGGCCACAGCTGTGCAGCCAGGACAGGTGGGAGTGTGGGGATCCAGGTAA
Paxip$^{+/+}$ CTGGGGTATGGATACGCAGAAGGAACAGGGGCAGGTTAGAATGAAGGATGGGCATCCCG
Paxip$^{+/+}$ GAAAAGATGTTTTTAGTTTTTATAGAATCGGGTAAGCAGGAACAGGTGGAAGTGTAG
Paxip$^{+/+}$ CAGTAAATGTACTTCCTGGTTACAGAGAAGCTGAGGCAGGT

	Paxip$^{+/+}$	*Paxip*$^{\Delta/\Delta}$
Blunt	6	6
1bp overlap	0	1
2bp overlap	1	2
3bp overlap	0	1
4bp overlap	0	0
5bp overlap	1	0
additions	6	7

Supplementary Figure 13

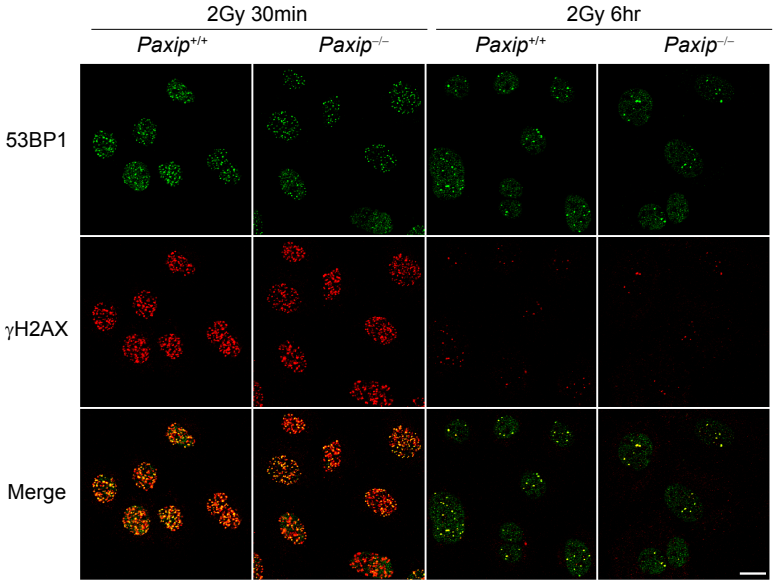

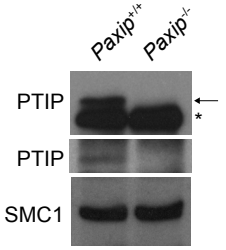

Supplementary Figure 14

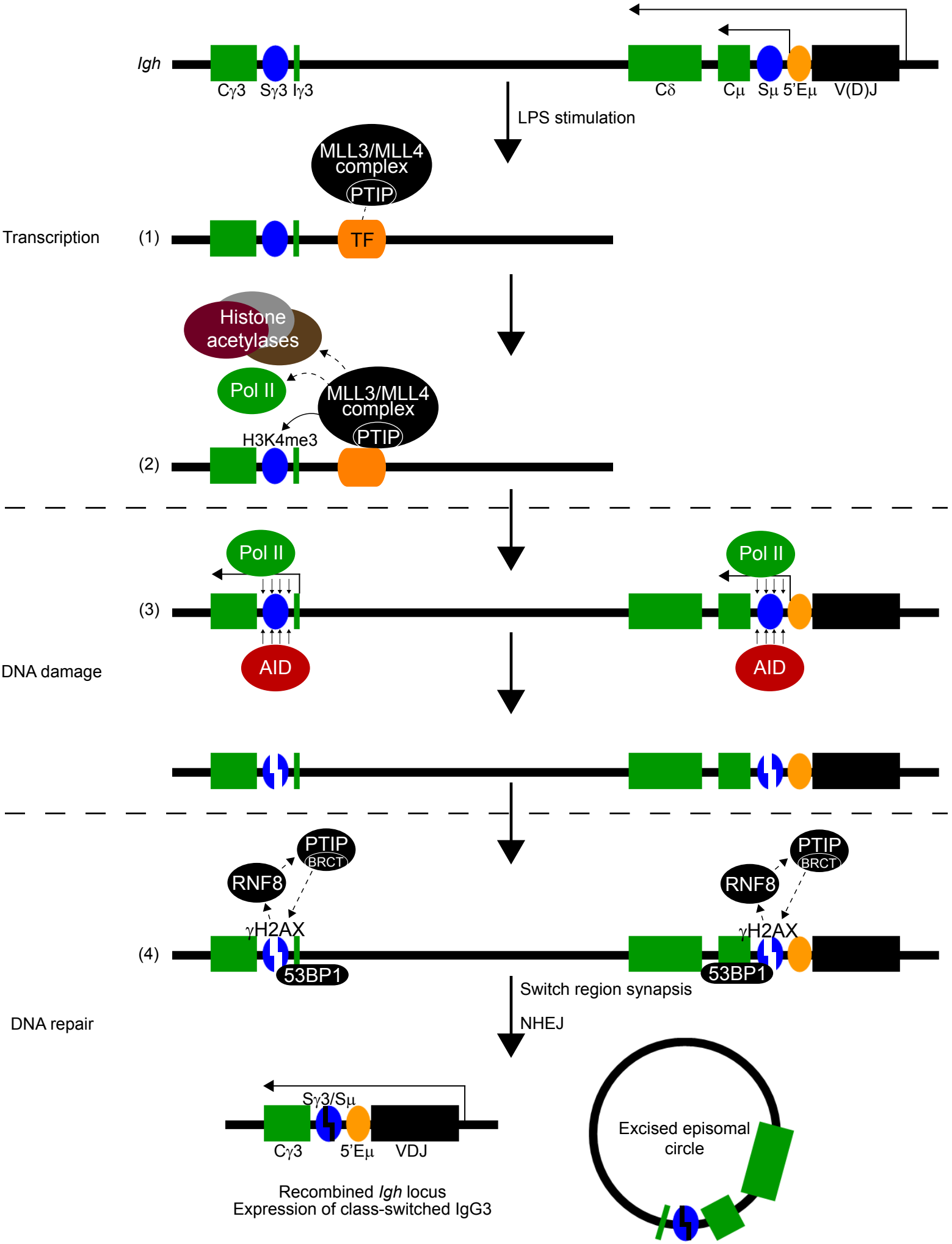

Supplementary Figure 15

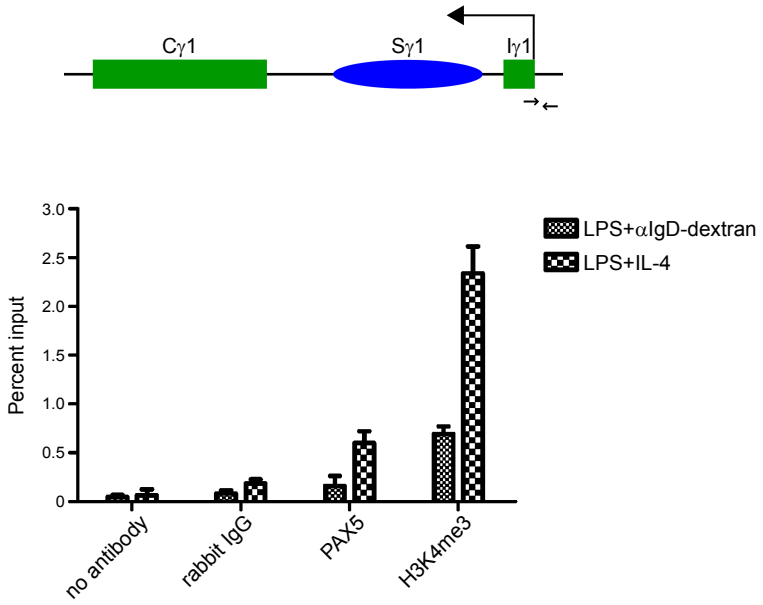

Supplementary Figure 16

Genotype	Stimulation	Antibody	Tag (millions)	Source	Catalog #
WT	none	H3K4me3	4.84	Millipore	17-614
WT	none	PTIP	10.41	Refs. S3&S4	
WT	LPS+αIgD-dextran	H3K4me1	3.57	Abcam	ab8895
WT	LPS+αIgD-dextran	H3K4me2	2.59	Abcam	ab7766
WT[1]	LPS+αIgD-dextran	H3K4me3	2.71		
WT[2]	LPS+αIgD-dextran	H3K4me3	3.77		
WT[3]	LPS+αIgD-dextran	H3K4me3	9.93		
WT	LPS+αIgD-dextran	H2BK5ac	14.40	Abcam	ab40886
WT	LPS+αIgD-dextran	H3K27ac	11.64	Abcam	ab4729
WT	LPS+αIgD-dextran	H3K36me3	13.35	Abcam	ab9050
WT	LPS+αIgD-dextran	H3K9ac	11.23	Abcam	ab4441
WT	LPS+αIgD-dextran	H4K8ac	13.37	Upstate	07-328
WT	LPS+αIgD-dextran	Pol II	11.50	Abcam	ab5408
WT	LPS+αIgD-dextran	PTIP	9.45		
WT	LPS+αIgD-dextran	rabbit IgG	10.32	Millipore	12-370
WT	LPS+αIgD-dextran	ASH2	10.31	Bethyl	A300-489A
WT	LPS+IL4	H3K4me3	14.06		
KO	none	PTIP	11.33		
KO	LPS+αIgD-dextran	H3K4me1	4.50		
KO	LPS+αIgD-dextran	H3K4me2	3.54		
KO[1]	LPS+αIgD-dextran	H3K4me3	3.29		
KO[2]	LPS+αIgD-dextran	H3K4me3	4.19		
KO[3]	LPS+αIgD-dextran	H3K4me3	11.14		
KO	LPS+αIgD-dextran	H2BK5ac	13.95		
KO	LPS+αIgD-dextran	H3K27ac	11.37		
KO	LPS+αIgD-dextran	H3K36me3	12.76		
KO	LPS+αIgD-dextran	H3K9ac	12.00		
KO	LPS+αIgD-dextran	H4K8ac	11.30		
KO	LPS+αIgD-dextran	Pol II	7.87		
KO	LPS+αIgD-dextran	PTIP	8.17		
KO	LPS+IL4	H3K4me3	7.20		

Supplementary Table 2

REFERENCES

S1. D. Kim, M. Wang, Q. Cai, H. Brooks, G. R. Dressler, *J Am Soc Nephrol* 18, 1458 (May, 2007).
S2. R. C. Rickert, J. Roes, K. Rajewsky, *Nucleic Acids Res* 25, 1317 (Mar 15, 1997).
S3. Y. W. Cho *et al.*, *Cell Metab* 10, 27 (Jul, 2009).
S4. Y. W. Cho *et al.*, *J Biol Chem* 282, 20395 (Jul 13, 2007).
S5. S. Difilippantonio *et al.*, *Nat Cell Biol* 7, 675 (Jul, 2005).
S6. K. M. McBride *et al.*, *J Exp Med* 205, 2585 (Oct 27, 2008).
S7. B. Reina-San-Martin *et al.*, *J Exp Med* 197, 1767 (Jun 16, 2003).
S8. E. Callen *et al.*, *Cell* 130, 63 (Jul 13, 2007).
S9. A. Barski *et al.*, *Cell* 129, 823 (May 18, 2007).
S10. Z. Wang *et al.*, *Nat Genet* 40, 897 (Jul, 2008).
S11. C. Zang *et al.*, *Bioinformatics* 25, 1952 (Aug 1, 2009).
S12. Z. Wang *et al.*, *Cell* 138, 1019 (Sep 4, 2009).
S13. J. Yuan, R. B. Crittenden, T. P. Bender, *J Immunol* 184, 2793 (Mar 15, 2010).
S14. C. C. Chu, W. E. Paul, E. E. Max, *Proc Natl Acad Sci U S A* 89, 6978 (Aug 1, 1992).
S15. E. A. Cho, M. J. Prindle, G. R. Dressler, *Mol Cell Biol* 23, 1666 (Mar, 2003).
S16. S. R. Patel, D. Kim, I. Levitan, G. R. Dressler, *Dev Cell* 13, 580 (Oct, 2007).
S17. M. Fang *et al.*, *Development* 136, 1929 (Jun, 2009).
S18. M. G. Guenther, S. S. Levine, L. A. Boyer, R. Jaenisch, R. A. Young, *Cell* 130, 77 (Jul 13, 2007).
S19. T. Y. Roh, S. Cuddapah, K. Cui, K. Zhao, *Proc Natl Acad Sci U S A* 103, 15782 (Oct 24, 2006).
S20. J. Stavnezer, J. E. Guikema, C. E. Schrader, *Annu Rev Immunol* 26, 261 (Apr, 2008).
S21. M. S. Lechner, I. Levitan, G. R. Dressler, *Nucleic Acids Res* 28, 2741 (Jul 15, 2000).
S22. J. Stavnezer, *Curr Top Microbiol Immunol* 245, 127 (2000).
S23. C. Cobaleda, A. Schebesta, A. Delogu, M. Busslinger, *Nat Immunol* 8, 463 (May, 2007).
S24. F. Liao, B. K. Birshtein, M. Busslinger, P. Rothman, *J Immunol* 152, 2904 (Mar 15, 1994).
S25. Y. Wakatsuki, M. F. Neurath, E. E. Max, W. Strober, *J Exp Med* 179, 1099 (Apr 1, 1994).
S26. A. J. Ruthenburg, H. Li, D. J. Patel, C. D. Allis, *Nat Rev Mol Cell Biol* 8, 983 (Dec, 2007).
S27. T. Hung *et al.*, *Mol Cell* 33, 248 (Jan 30, 2009).
S28. M. Vermeulen *et al.*, *Cell* 131, 58 (Oct 5, 2007).
S29. C. Jiang, B. F. Pugh, *Nat Rev Genet* 10, 161 (Mar, 2009).

Supporting Online Material
www.sciencemag.org
Materials and Methods
Supplemental Results and Discussion
Figures S1-S16
Tables S1, S2
References